Original Research

Prediction of overall survival and response to immune checkpoint inhibitors: An immune-related signature for gastric cancer ☆,☆☆

Zheng Wang [a,b], Xiang Li [d], Ying Xu [a,c,*]

[a] *Shanghai University of Traditional Chinese Medicine, No. 1200, Cailun Road, 200120 Shanghai, China*
[b] *Shuguang Hospital Affiliated to Shanghai University of Traditional Chinese Medicine, Shanghai, China*
[c] *Laboratory of TCM Four Processing, Shanghai University of Traditional Chinese Medicine, Shanghai, China*
[d] *Hebei Agricultural University, Hebei, China*

A B S T R A C T

Gastric cancer (GC) is common in East Asia and South and Central America. Most GC patients miss the opportunities for surgery. Despite their therapeutic potential, immune checkpoint inhibitors (ICIs) only work in part of patients with GC. Thus, this study was aimed at constructing a signature for diagnosis, prognosis, and prediction of response to ICIs. A multivariate analysis showed that the 8-immune-related-gene (IRG) signature was an independent prognostic factor of overall survival among GC patients. In the high-risk group of 8IRG signature risk score, the fractions of CD4 T cells, macrophage M2 and monocyte, which is associated with the progression of cancers, were higher. The low-risk group had a higher immunophenoscore, which meant a better response to ICIs.

Introduction

Gastric cancer (GC) locates on gastric mucosa epithelium, with the highest incidence in East Asia and South and Central America. The rate ranks first of the malignant tumor among men in Japan and Korea. GC is also a leading cause of cancer death in China [1]. More than 90% of GC is adenocarcinoma without dramatic symptoms, for which patients miss the surgery opportunities when diagnosed [2]. The 5-year survival rate of patients with advanced GC is no more than 20%. Thus, an early diagnostic method and a novel treatment for GC are necessary.

Immune checkpoint inhibitors (ICIs), which are related to tumor immune microenvironment and immune escape, provide a new way for tumor therapy. ICIs function well in non-small cell lung cancer [3], renal cell cancer [4], colorectal cancer [5] and melanoma [6]. Based on this, studies also showed that immune-related genes had potential to be biomarkers for cancer diagnosis and prognosis.

However, not all GC patients benefit from ICIs [7,8]. It remains a problem to solve that which patients respond well to ICIs and which don't. Additionally, despite of the potential, a single gene can hardly act as a capable prediction factor.

This study is aimed at developing an immune related signature for GC diagnosis and prognosis. Besides, clinical phenotype, immune cell infiltration, mutation data, and prediction for response to ICIs would be investigated. This may contribute to the diagnosis and prognosis of GC as well as in clinical decisions.

Materials and methods

Fig. 1 presented the flowchart of the whole study.

Patient data

GC datasets of normal samples and tumor samples were downloaded from The Cancer Genome Atlas (TCGA) data portal (https://portal.gdc.cancer.gov/); and datasets of normal samples were downloaded from Genotype-Tissue Expression (GTEx) portal (https://gtexportal.org/home/) for comparison. In addition, a gene list was downloaded to identify immune-related genes (details in references) [9].

Differentially expressed genes analysis

We screened differentially expressed genes (DEGs) between the normal samples and the tumor samples mentioned above via limma package [10] in R. Adjusted *P*-value < 0.05 and |log2 (fold change) | >1 were set as the thresholds. Then the intersection of the DEGs and the listed immune-related genes was selected as differentially expressed immune-related genes (DE-IRGs).

Calculation and validation of the immune-related signature of GC

The GC patients from TCGA were divided into a training (TRN) set and a testing (TST) set at a ratio of 7:3. The TRN set would be used to

---
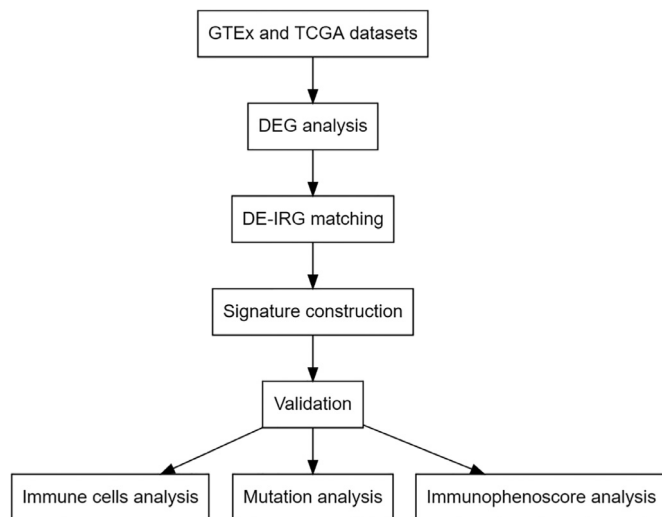
Fig. 1. Overall flowchart of this study.

Fig. 2. Venn diagram for the intersections of GC differentially expressed genes and immune-related genes.

proportional hazard regression analysis to identify the significant variables for GC survival. If $P < 0.05$, the corresponding DE-IRGs were considered as prognostic ones. And the least absolute shrinkage and selection operator (LASSO) penalized Cox proportional hazards regression was applied for overfitting minimization via glmnet package [11]. We would choose the variables under min lambda, which gave minimum mean cross-validated error, for usability of the signature. Furthermore, the signature would be constructed via multivariate Cox proportional hazard regression analysis. The signature would be calculated with the following model for each patient: Risk score = expression 1 * coefficient
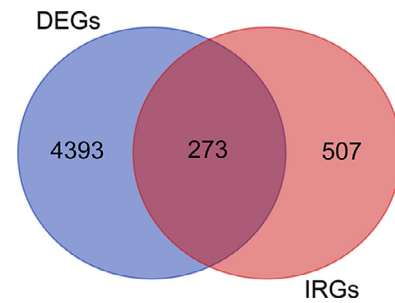
construct the immune-related signature of GC, and the TST set would be used to valid the power of this signature. We used a univariate Cox

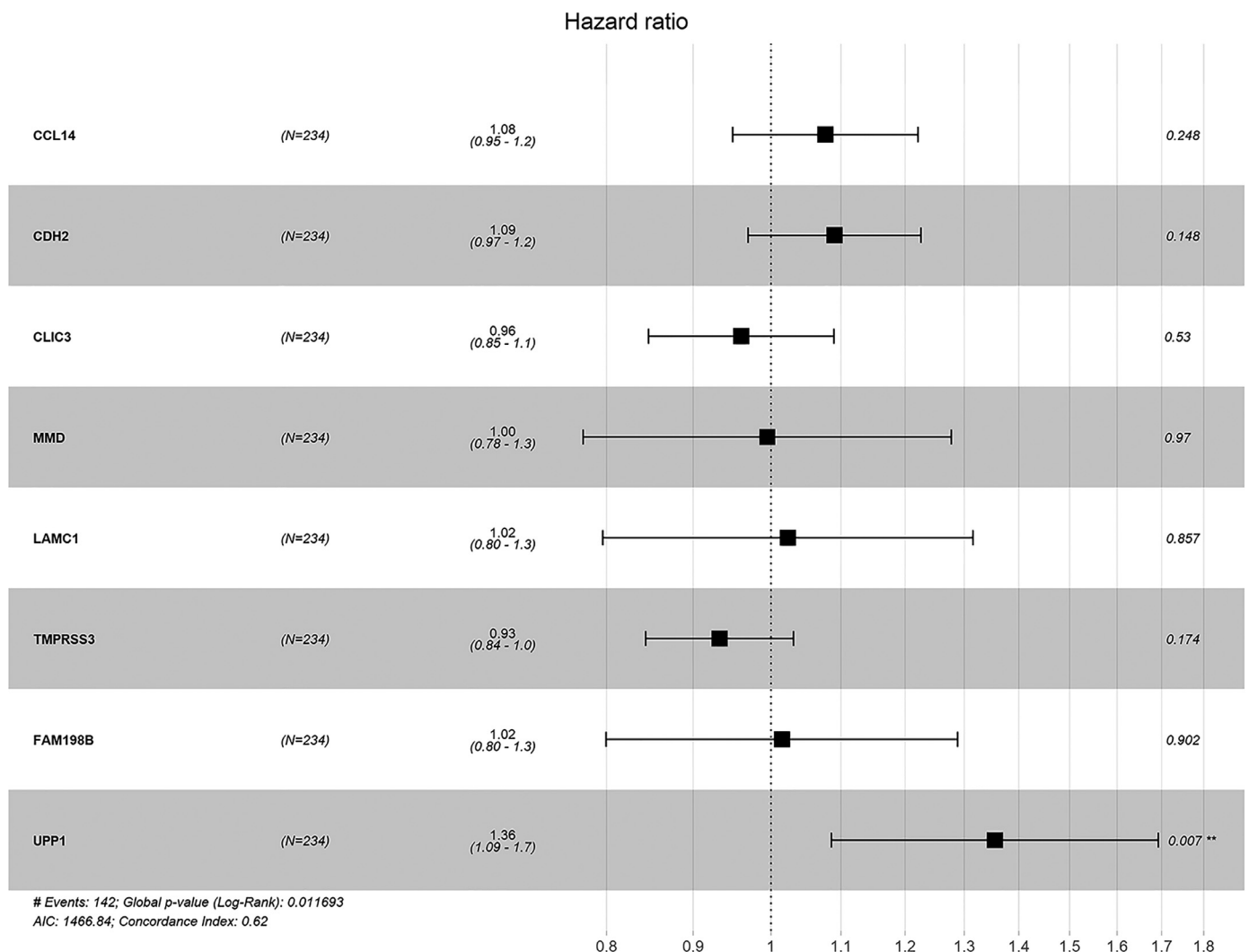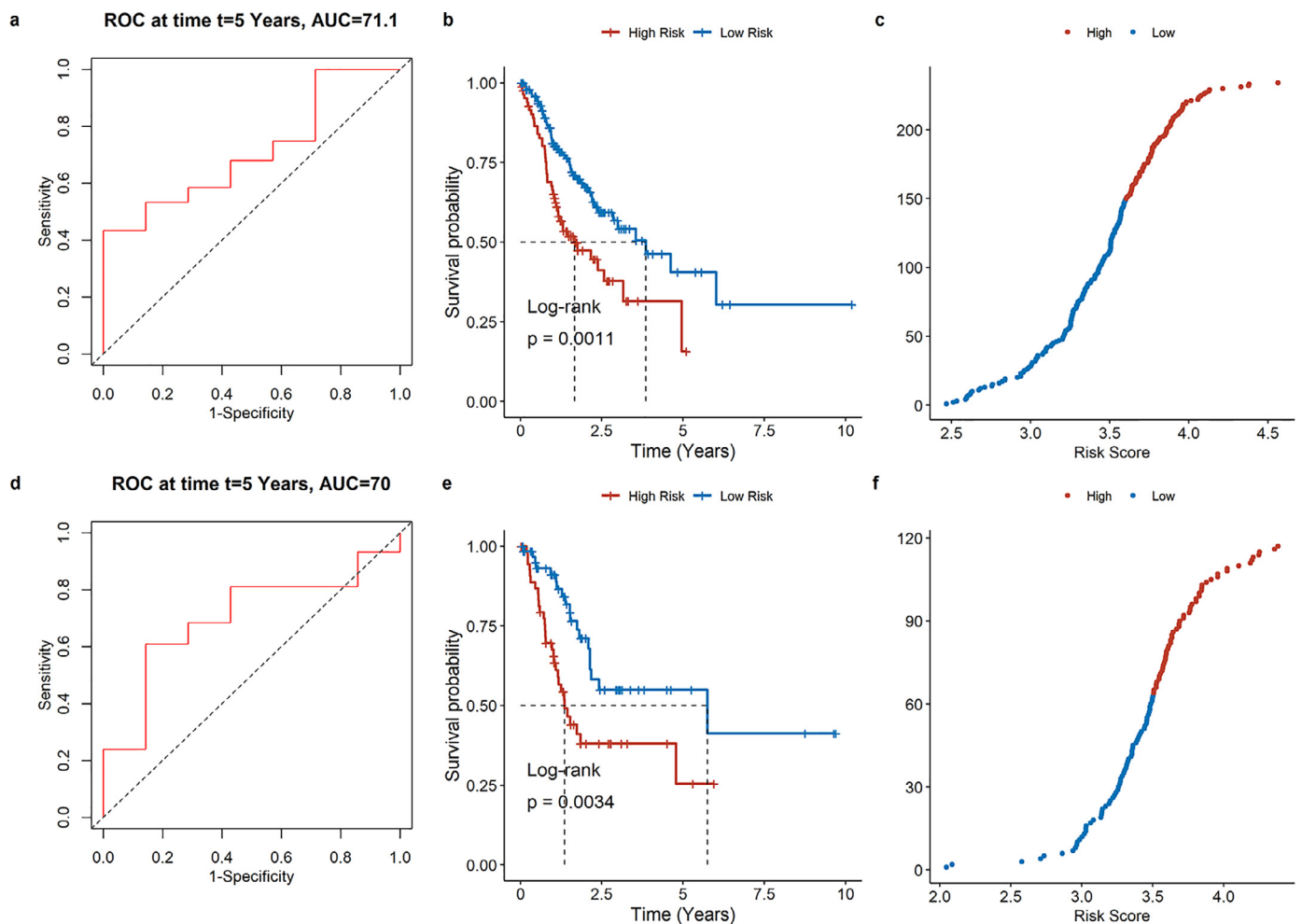Fig. 3. Forest plot of the 8 IRGs in the multivariate cox analysis.

Fig. 4. Identification of the 8-IRG signature in the 2 sets. (a)Time-dependent ROC curves analysis of TRN set. (b) Kaplan-Meier curve analysis of overall survival of GC patients in TRN set. (c)Risk score distribution in TRN set. (d)Time-dependent ROC curves analysis of TST set. (e) Kaplan-Meier curve analysis of overall survival of GC patients in TST set. (f)Risk score distribution in TST set.

1 + expression 2 * coefficient 2 + … + expression n * coefficient n. The receiver operating characteristic curve (ROC) would be plotted both in TRN and TST sets via timeROC package to validate the prognostic capability of the signature. Then the patients would be divided into high-risk and low-risk groups in their own set according to the sensitivity ROC. The final step in this section, we would plot the Kaplan–Meier survival curves of the high-risk and low-risk groups via survival package, which could demonstrate the comparison of survival possibility between the two groups.

Estimate of tumor-infiltrating immune cells

The Cancer Immunome Atlas (TCIA, https://tcia.at/home) is an online platform that stores immune-related data of samples from TCGA and other data sources. We would download the cellular composition of immune infiltration data of each sample from this platform and calculated the relationship between the signature and the infiltration.

Mutation analysis

The mutation data (stored in MAF form) of GC tumor samples would be downloaded from TCGA and be analyzed via maftools package [12]. And we would calculate the tumor mutation burden (TMB) score of each GC patient as follows: TMB= (total mutation/total covered bases) $\times 10^6$ [13].

Immunophenoscore analysis

In this section, we would further compare the expression of PD1 and related genes, the immunophenoscore (IPS), and the response to ICIs from TCIA so that we could observation between the immune microenvironment and the signature. IPS reflects the immune microenvironment of the patients, and IPS-PD1/PD-L1/PD-L2 reflects the potential respond to the corresponding blockers.

Results

Patient characteristics

We obtained the RNA-seq data of 356 normal samples and 373 tumor samples, of which 351 tumor ones had matched clinical data. We randomly divided the 351 patients into the TRN set ($n = 234$) and the TST set ($n = 117$). There was no statistical difference of the general characteristics between the two sets (Table 1).

Identification of DE-IRGs

According to the threshold mentioned above, 4666 DEGs in total were identified, consisting of 3748 up-regulated ones and 918 down-regulated ones. Then we extracted 273 DE-IRGs (Fig. 2).

Table 1
General characteristics of the patients.

	Training Set	Testing Set	P Value	Method
Gender			0.77	Pearson's Chi-squared Test
Female	111	46		
Male	197	87		
Age	66±10	65±11	0.78	Wilcoxon Rank Sum Test
Race			0.32	Fisher's Exact Test
Asian	68	21		
BoAA	10	3		
NHoOPI	1	0		
White	46	16		
NR	183	93		
Stage			0.32	Pearson's Chi-squared Test
Stage I	39	20		
Stage II	97	33		
Stage III	119	63		
Stage IV	33	10		
NR	20	7		
T Stage			0.88	Fisher's Exact Test
T1	16	7		
T2	62	31		
T3	183	58		
T4	92	35		
TX	8	2		
N Stage			0.19	Fisher's Exact Test
N0	94	38		
N1	81	37		
N2	56	28		
N3	62	26		
NX	15	2		
NR	0	2		
M Stage			0.99	Pearson's Chi-squared Test
M0	265	125		
M1	20	9		
MX	15	7		
Grade			0.91	Fisher's Exact Test
G1	8	4		
G2	112	45		
G3	182	81		
GX	6	3		

Note: BoAA: black or African American; NHoOPI: native Hawaiian or other Pacific islander; NR: not reported.

Table 2
Result of the univariate Cox.

Gene Symbol	Log2 (FC)	Adj. P
ADAM12	1.583	1.46E-74
ADAMTS12	1.682	7.58E-61
BCL11B	1.552	3.23E-102
CCL14	−3.054	2.18E-62
CD36	−1.524	1.47E-34
CDA	1.825	9.32E-33
CDH2	−1.225	3.84E-32
COL4A1	2.253	1.84E-58
CXCR4	1.603	1.26E-41
DAB2	1.196	8.76E-26
RGS1	1.806	3.42E-39
NRP1	1.327	7.86E-33
LGALS1	1.092	3.12E-09
MMD	1.221	8.46E-28
FN1	1.873	6.68E-12
F13A1	−1.205	7.01E-18
LAMC1	1.151	2.05E-09
GLIPR1	1.164	3.65E-17
FSTL1	1.347	5.78E-12
FAM198B	1.657	2.64E-37
GPR183	1.005	6.70E-18
FZD2	1.599	3.07E-72
UPP1	1.114	2.72E-26
SELL	1.878	3.46E-49

in the low-risk group ($P = 0.0011$, Fig. 4b). The risk scores of the patients in the TRN set were ranked, and we plotted their distribution in Fig. 4c. The heatmap revealed expression comparison of 8 DE-IRGs between two risk groups (Fig. 5).

In order to valid the stability of the 8-IRG signature, we further verified its prognostic capability in the TST set. The risk scores of each patient were calculated as well and the AUC is 70 (Fig. 4d). After grouping, there were 54 patients in the high-risk group and 65 ones in the low-risk group. Similarly, overall survival of the high-risk patients was poorer than that of the low-risk ones (Fig. 4e). And the distribution of the patients and the expression heatmap of 8 DE-IRGs were presented in Figs. 4f and 5.

Association between the signature and clinical factors

We analyzed the association between the immune signature and clinical pathological variables. Significant differences were observed in T stage and N stage but not in tumor burden, M stage, N stage, grade, and clinical stage (Fig. 6). In addition, among the molecular subtypes of GC, genomically stable subtype got the highest risk score while Epstein-Barr virus subtype got the lowest (Fig. 6).

Tumor immune microenvironment changing associated with the signature

Immune cells play an important role of tumor immune microenvironment. Thus, we tried to figure out which classes of immune cells were linked to the 8-IRG risk signature. TCIA could assess the relative proportion of the 10-type immune cells according to the RNA-sequencing data. Fig. 7 presented the immune cell type abundance between the 8-IRG signature low-risk group and the high-risk group from the total set. Among the 10 immune cell types, CD4 T cells, macrophage M2 and monocyte were significantly associated with the risk score (Fig. 7).

The signature and the mutation profile

We estimated the association between mutation profile and the signature of the GC patients (Fig. 8). The top 5 mutated genes in the high-risk group were TP53, CSMD3, LRP1B, FLG and SYNE1. And those in the low-risk group were TP53, SYNE1, LRP1B, ARID1A and CSMD3. Unexpectedly, the TMB in the high-risk group was lower than that in the low-risk group.
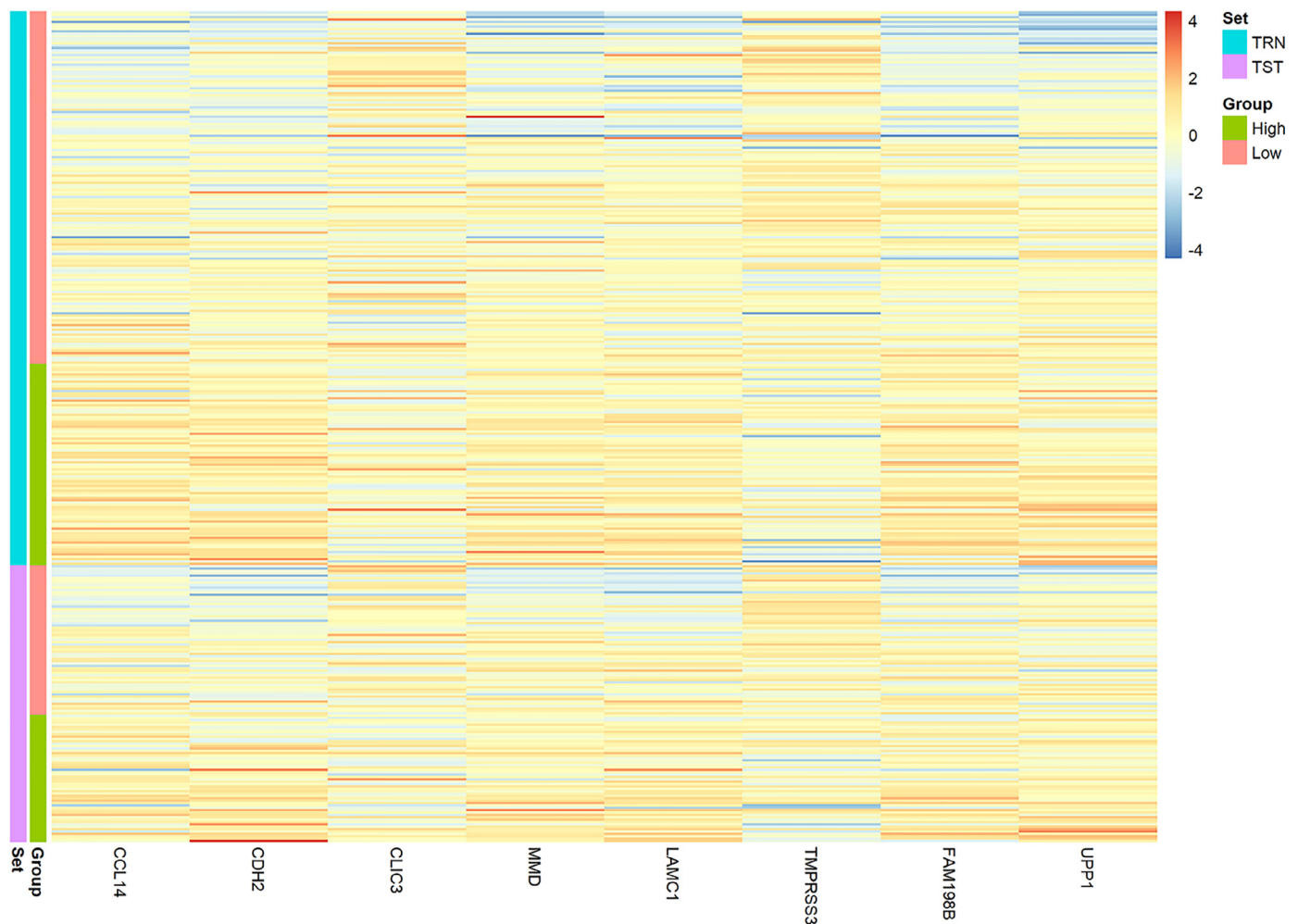
Construction of the signature

We performed a univariate Cox regression analysis in the TRN set to investigate the prognostic value of the 273 DE-IRGs. 24 DE-IRGs were significantly associated with the overall survival of GC patients in the TRN set (Table 2). The 24 DE-IRGs underwent LASSO analysis to minimize overfitting, and 8 of the 12 DE-IRGs were identified. Then we used the 8 DE-IRGs to construct the immune signature (Fig. 3). The signature for prediction was defined as a linear combination of the expression levels of the 8 DE-IRGs weighted by their relative coefficient in the multivariate Cox regression as follows: risk score= 0.07401^* CCL14+0.08644^*CDH2−0.04041^*CLIC3−0.00487^*MMD+0.02315^*LAMC1−0.06966^*TMPRSS3+0.01500^*FAM198B+0.30403^*UPP1. Three (CLIC3, MMD and TMPRSS3) of the 8 DE-IRGs were linked to high risk and five (CCL14, CDH2, LAMC1, FAM198B and UPP1) were protective ones.

We calculated the risk scores of each patient in the TRN set based on the above signature. The AUC of the 8-immune-related-gene (8-IRG) signature was 71.1 at 5-year survival (Fig. 4a). Then the patients were divided into high-risk ($n = 85$) and low-risk ($n = 149$) groups according to the ROC. High-risk patients had a poorer overall survival than those

Fig. 5. The heatmap of 8 IRGs between two groups in TRN set and TST set. High stands for high-risk group and Low stands for low-risk group.

The signature and the response to ICI

The relationship between IPS and the 8-IRG risk signature was investigated in our study (Fig. 9). Though there was a significant difference in expression between the two groups ($P<0.001$) only, the IPS ($P<0.01$) and the IPS-PD1/PD-L1/PD-L2 ($P<0.001$) of the low-risk group is higher than that of the high-risk group, which means the patients in the low-risk group could have better response to ICIs.

Discussion

Studies have shown that ICIs have potential in the treatment for GC. However, they don't have effect on all patients. So, it's important to identify a biomarker for ICIs. Single-gene biomarkers have the disadvantages of low sensitivity and low specificity. Thus, signatures made up of several variables seems increasingly valuable.

We used the data from GTEx and TCGA to construct and validate the IRG signature, which consisted of 8 prognostic DE-IRGs. Three (CLIC3, MMD and TMPRSS3) of the 8 genes were related to high risk, while five (CCL14, CDH2, LAMC1, FAM198B and UPP1) were protective factors. Compared to the normal samples, 3748 genes were up-regulated in the tumor samples, and 918 were down-regulated.

Some of the 8 genes were reported to play important roles in the development and prognosis of cancers.

It was found that CLIC3 expression was higher in the resected pancreatic cancer specimens than in the precursor lesions known as pancreatic intraepithelial neoplasms [14]. However, in pancreatic intraep-ithelial neoplasms lesions, CLIC3 expression increased with higher degrees of dysplasia compared to well-organized epithelia lesions. In a survival analysis, high expression of CLIC3 was a strong prediction factor of poor survival. CLIC3 is considered to play a role in tumor invasiveness through a Rab25 dependent mechanism, which is essential for integrin recycling [14].

About 20 years ago, TMPRSS3 was found overexpressing in ovarian cancer and was introduced as a potential therapeutic biomarker. The transcription and protein levels of TMPRSS3 were significantly increased in epithelial ovarian cancer as compared to normal ovarian epithelium cells and low malignant potential ovarian tumors [15]. In an immunohistochemical study comparing breast cancer tissue samples with adjacent normal tissue, TMPRSS3 expression was significantly increased in tumor tissue. The expression level of TMPRSS3 was also associated with disease stage, lymph node metastasis, and proliferation of the cancer cells [15].

CCL14 has both anti- and pro-cancer properties. The expression of this chemokine is reduced in many solid tumors such as breast, lung, liver, and prostate cancer [16,17]. On the other hand, it is elevated in brain and esophageal cancer [18]. CCL14 reduces the activation of the Wnt/β-catenin pathway in HCC cells, thereby inhibiting their proliferation and leading to HCC cells apoptosis. CCL14 also has pro-cancer properties. Experiments on breast cancer cells have shown that it could induce the migration of cancer cells and also cause angiogenesis. It is also reported that the CCL14-CCR1 axis is crucial in liver metastasis [18].
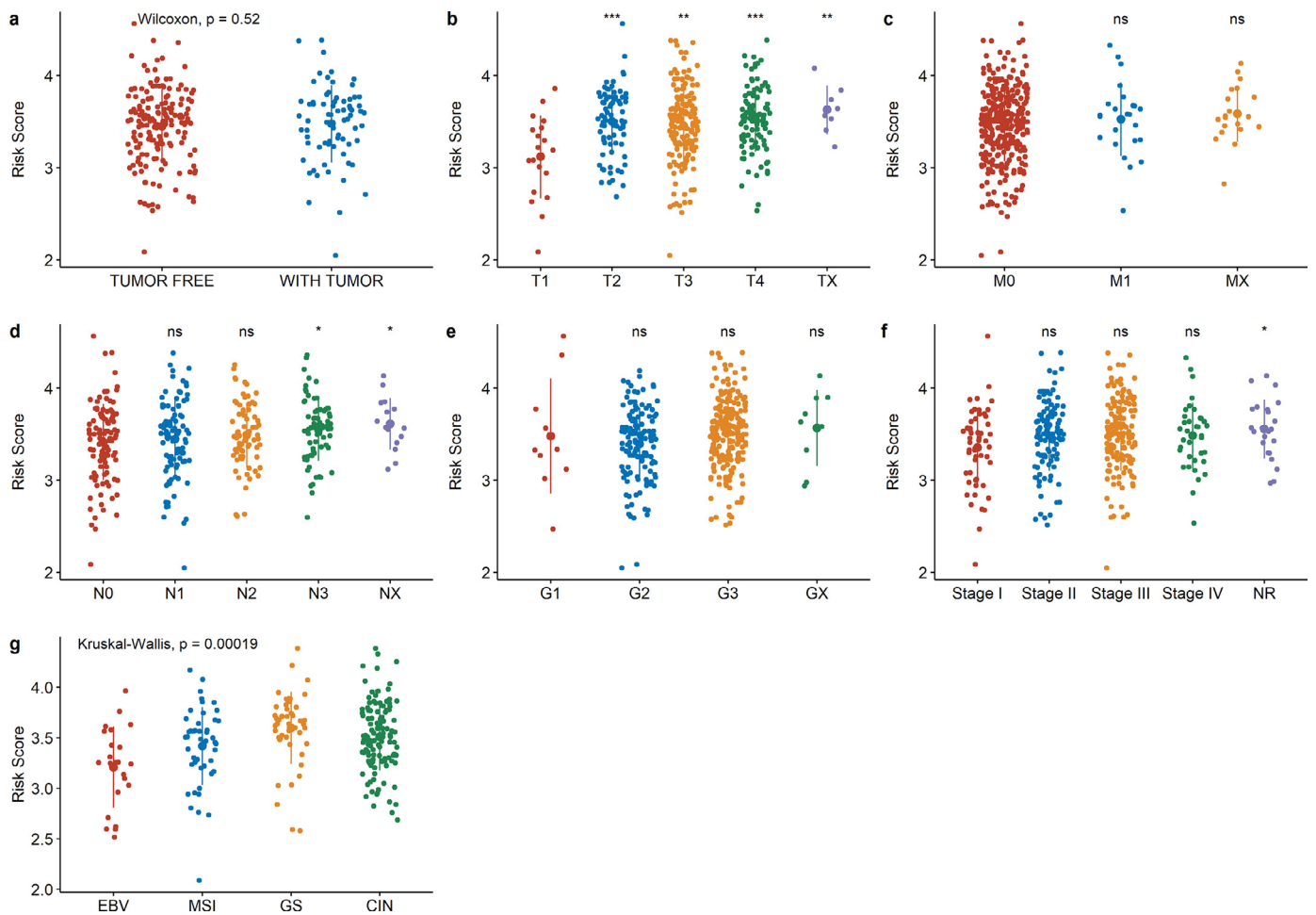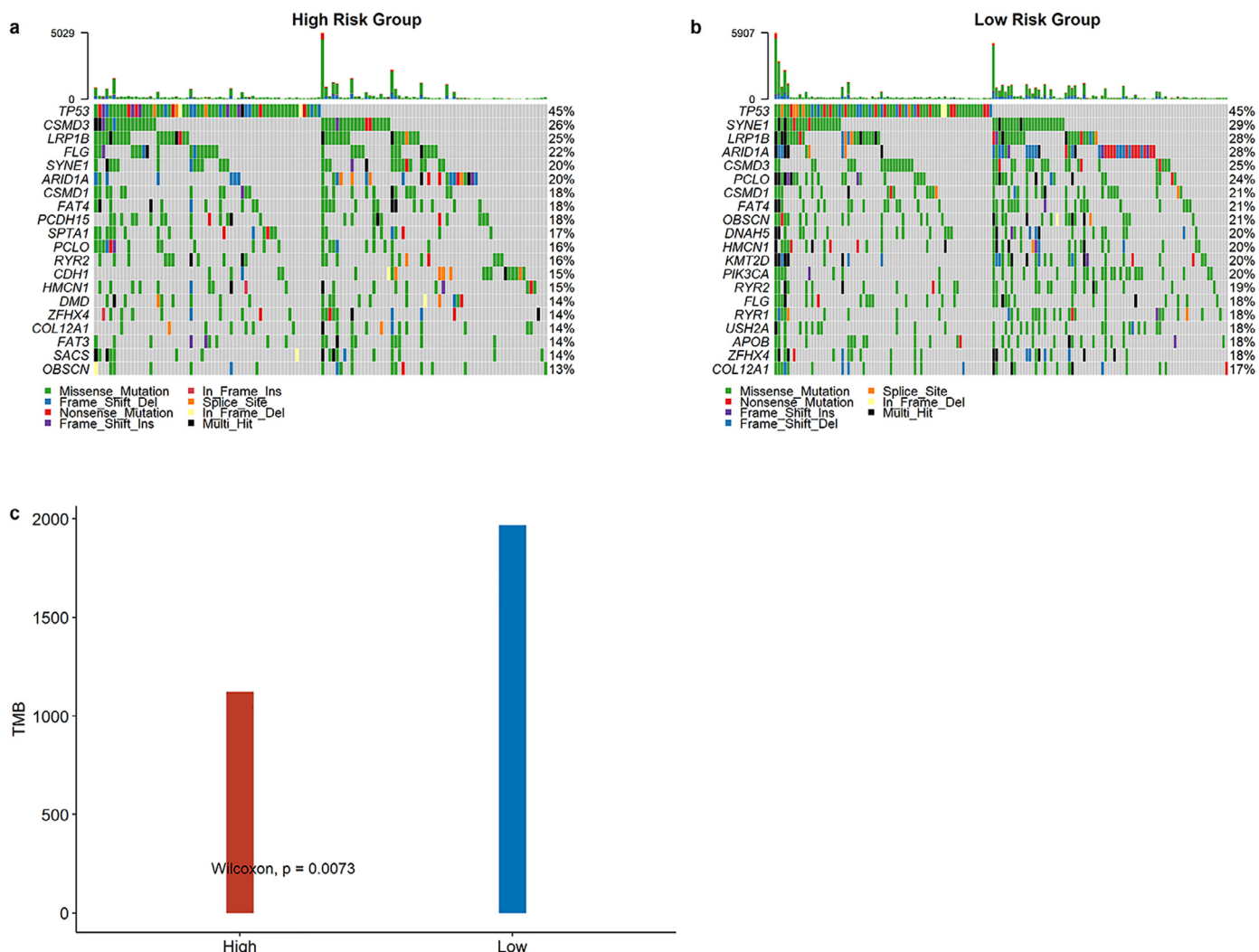
Fig. 6. The relationships between the signature and (a) tumor burden; (b) T stage; (c) M stage; (d) N stage; (e) grade; and (f) clinical stage; (g) molecular subtype. *$P<0.05$; **$P<0.01$; ***$P<0.001$; ns: not significant. Reference group: (b) T1; (c) M0; (d) N0; (e) G1; (f) Stage I.

We may suppose that the genetic changes of tumor immune environment in high-risk GC patients contributes to the poor survival. Because of the significant difference in the survival curves, the signature revealed a good prognostic power. Moreover, the signature was significantly associated with the survival possibility of the GC patients. The results showed that the signature is a reliable prognostic tool. The relationship between the signature and several pathological factors showed

that this signature was not affected by tumor burden, M stage, grade, and clinical stage. The results confirmed that the signature is a reliable prognostic tool. In addition, it is known that GC is divided into four subtypes, namely Epstein-Barr Virus positive (EBV) type, microsatellite instability (MSI) type, genomically stable (GS) type, and chromosomally instability (CIN) type [19]. Among them, EBV type displays recurrent PIK3CA mutations, extreme DNA hypermethylation, and amplification
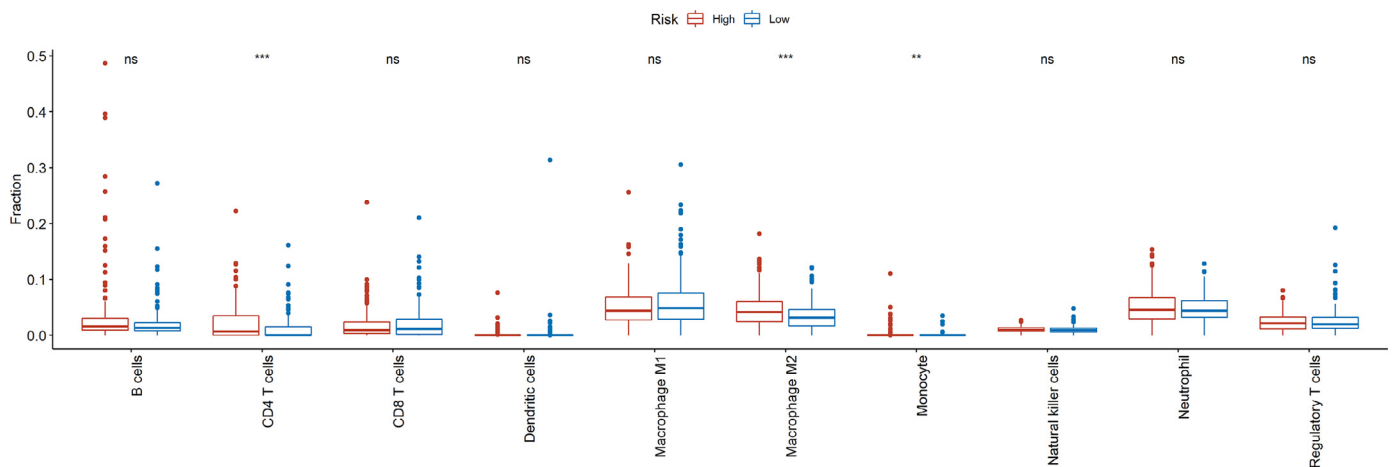
Fig. 7. The association of immune cells infiltration and the signature in GC. *$P<0.05$; **$P<0.01$; ***$P<0.001$; ns: not significant.

Fig. 8. The mutation profile and TMB between high-risk and low-risk groups. (a) Mutation profile of high-risk groups; (b) Mutation profile of low-risk groups; (c) The relationship between the immune related risk signature and TMB.

of JAK2, CD274 (namely PD-L1) and PDCD1LG2 (namely PD-L2). Interestingly, the EBV group got the lowest risk score of our signature. This also may explain why our signature is potentially associated with ICI-respond prediction.

Furthermore, we estimated the relative proportions of 10-type immune cells of each GC sample. The abundance of CD4 T cells, macrophage M2 and monocyte were high in the high-risk group, which seemed to be an explanation for the prognostic power of the signature. It is known that CD4+ T cells are essential organizers of cell-mediated immunity, participating in every stage of the immune response [20]. Naive CD4+ T cells can be induced to differentiate to specific lineages according to the local cytokine milieu, towards Th1, Th2, Th17 and Treg and Th17 cells with both anti-tumor and pro-tumor functions in different cancers [20]. A study using peritoneal macrophage showed that M2 macrophages produce anti-inflammatory cytokines, such as TGF-β and IL-10 [21]. IL-10 may trigger activation of the T-cell-inhibitory receptor PD-L1 on tumor-associated macrophages, which favors the inhibition of tumor-specific T-cell immunity, and thus contributes to the general suppression of anti-tumor activities in the tumor environment [21].

In solid tumors such as NSCLC, melanoma or bladder cancer, TMB was assessed as a biomarker for ICIs based on the observation of successful immune checkpoint inhibition [22]. And in our study, the TMB of the low-risk group was significantly higher than that in the high-risk group, which meant the signature has the similar function with TMB to some degree.

We had explored the association between the IPS and the signature. The expression of PD-L2 was significantly higher in the high-risk group. The IPS and IPS-PD1/PD-L1/PD-L2 increased in the low-risk group compared to the high-risk group. It's suggested that the signature may represent the immunogenic tumor microenvironment of GC. Briefly, the patience with low risk score may have a better immune microenvironment and respond better to ICIs than the other group. We could suppose that GC patient with a lower risk score has a better response to ICIs.

In conclusion, we constructed a reliable immune related signature which can predict the survival and response to ICI of GC patient. This is a novel study of immune-related prognostic model based on RNA-seq, which estimated the relative proportion of 10-type immune cells of GC data from GTEx and TCGA. This signature was also used to explore the relationship among TMB, abundance of the immune cells, and prognosis. The signature would not be affected by most clinical phenotypes. In spite of the inspiring results, there are several limitations. The main one is that the signature was established on limited data from retrospective studies. Thus, data size of certain categories (such as stages) is small. More data on patients of different races will be necessary in further studies.
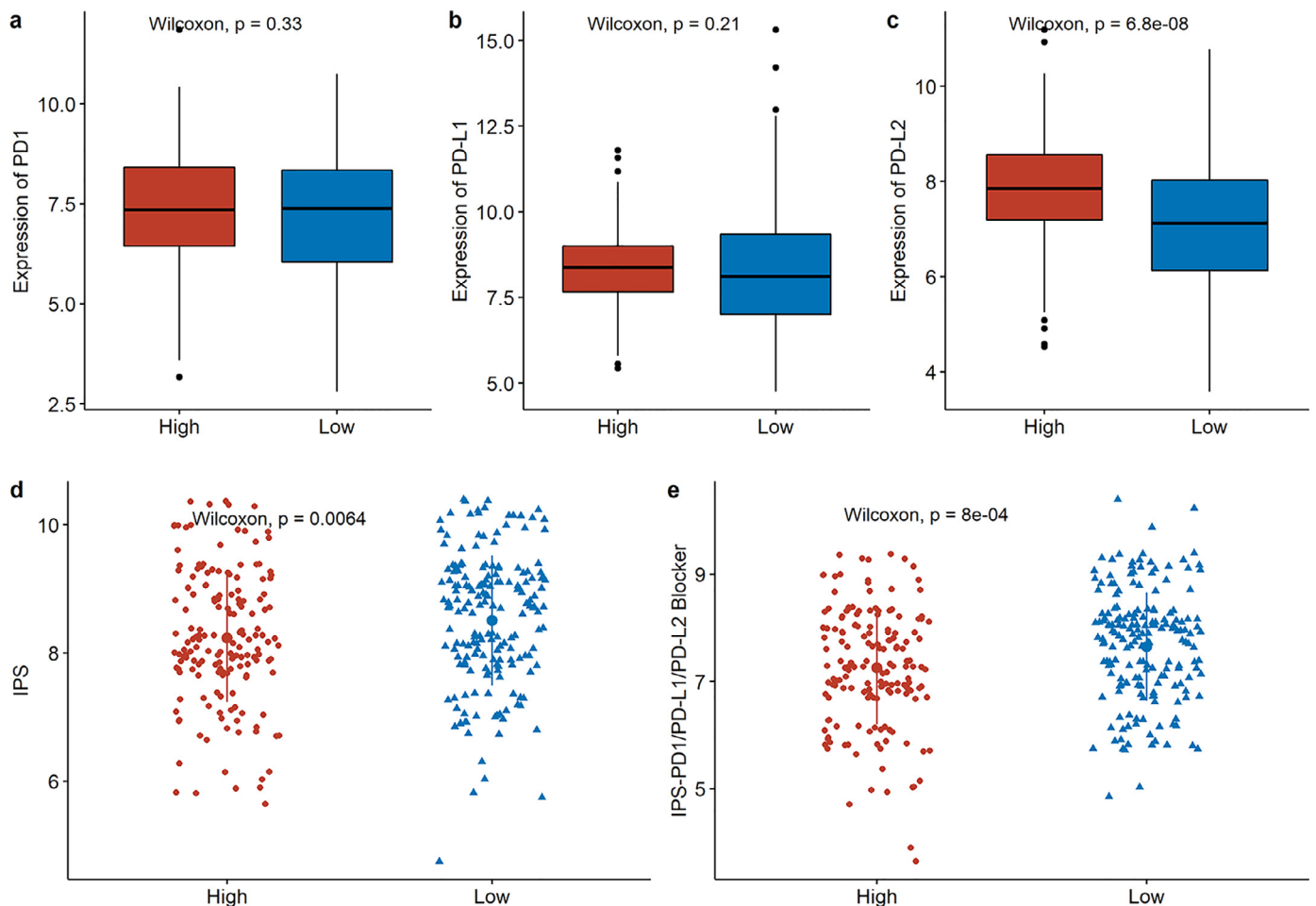
Fig. 9. IPS and immunotherapy gene expression analysis. (a) The gene expression of PD1 in high-risk and low risk groups. (b) The gene expression of PD-L1 in high-risk and low risk groups. (c) The gene expression of PD-L2 in high-risk and low risk groups. (d) The association between IPS and the immune related risk signature of GC patients. (e) The association between the response to PD1, PD-L1 and PD-L2 blockers, and the immune related risk signature of GC patients.

Data availability statement

The data used to support the findings of this study are included within the article.

Declaration of Competing Interest

The authors declare that they have no known competing financial interests or personal relationships that could have appeared to influence the work reported in this paper.

CRediT authorship contribution statement

Zheng Wang: Project administration, Supervision, Writing – original draft, Conceptualization, Investigation, Methodology, Supervision. **Xiang Li:** Data curtion, Formal analysis, Software, Visualization. **Ying Xu:** Funding acquisition, Writing – review & editing.

Reference

[1] L.A. Torre, R.L. Siegel, E.M. Ward, A. Jemal, Global cancer incidence and mortality rates and trends–an update, Cancer Epidemiol. Biomark. Prev. 25 (1) (2016) 16–27.

[2] J. Ma, H. Shen, L. Kapesa, S. Zeng, Lauren classification and individualized chemotherapy in gastric cancer, Oncol. Lett. 11 (5) (2016) 2959–2964.

[3] E.B. Garon, N.A. Rizvi, R. Hui, N. Leighl, A.S. Balmanoukian, J.P. Eder, et al., Pembrolizumab for the treatment of non-small-cell lung cancer, N. Engl. J. Med. 372 (21) (2015) 2018–2028.

[4] R.J. Motzer, B. Escudier, D.F. McDermott, S. George, H.J. Hammers, S. Srinivas, et al., Nivolumab versus everolimus in advanced renal-cell carcinoma, N. Engl. J. Med. 373 (19) (2015) 1803–1813.

[5] D.T. Le, J.N. Uram, H. Wang, B.R. Bartlett, H. Kemberling, A.D. Eyring, et al., PD-1 blockade in tumors with mismatch-repair deficiency, N. Engl. J. Med. 372 (26) (2015) 2509–2520.

[6] C. Robert, J. Schachter, G.V. Long, A. Arance, J.J. Grob, L. Mortier, et al., Pembrolizumab versus Ipilimumab in Advanced Melanoma, N. Engl. J. Med. 372 (26) (2015) 2521–2532.

[7] C. Chen, F. Zhang, N. Zhou, Y.M. Gu, Y.T. Zhang, Y.D. He, et al., Efficacy and safety of immune checkpoint inhibitors in advanced gastric or gastroesophageal junction cancer: a systematic review and meta-analysis, Oncoimmunology 8 (5) (2019) e1581547.

[8] M. Alsina, M. Moehler, C. Hierro, R. Guardeño, J. Tabernero, Immunotherapy for gastric cancer: a focus on immune checkpoints, Target Oncol. 11 (4) (2016) 469–477.

[9] P. Charoentong, F. Finotello, M. Angelova, C. Mayer, M. Efremova, D. Rieder, et al., Pan-cancer immunogenomic analyses reveal genotype-immunophenotype relationships and predictors of response to checkpoint blockade, Cell Rep. 18 (1) (2017) 248–262.

[10] M.E. Ritchie, B. Phipson, D. Wu, Y. Hu, C.W. Law, W. Shi, et al., limma powers differential expression analyses for RNA-sequencing and microarray studies, Nucl. Acids Res. 43 (7) (2015) e47.

[11] M. Fernández-Delgado, M.S. Sirsat, E. Cernadas, S. Alawadi, S. Barro,

M. Febrero-Bande, An extensive experimental survey of regression methods, Neural Netw. 111 (2019) 11–34.

[12] A. Mayakonda, D.C. Lin, Y. Assenov, C. Plass, H.P. Koeffler, Maftools: efficient and comprehensive analysis of somatic variants in cancer, Genome Res. 28 (11) (2018) 1747–1756.

[13] D.R. Robinson, Y.M. Wu, R.J. Lonigro, P. Vats, E. Cobain, J. Everett, et al., Integrative clinical genomics of metastatic cancer, Nature 548 (7667) (2017) 297–303.

[14] S.H. Patel, M.J. Edwards, S.A. Ahmad, Intracellular ion channels in pancreas cancer, Cell. Physiol. Biochem. 53 (S1) (2019) 44–51.

[15] C.E. Martin, K. List, Cell surface-anchored serine proteases in cancer progression and metastasis, Cancer Metastasis Rev. 38 (3) (2019) 357–387.

[16] M. Zhu, W. Xu, C. Wei, J. Huang, J. Xu, Y. Zhang, et al., CCL14 serves as a novel prognostic factor and tumor suppressor of HCC by modulating cell cycle and promoting apoptosis, Cell Death Dis. 10 (11) (2019) 796.

[17] Y. Gu, X. Li, Y. Bi, Y. Zheng, J. Wang, X. Li, et al., CCL14 is a prognostic biomarker and correlates with immune infiltrates in hepatocellular carcinoma, Aging (Albany NY) 12 (1) (2020) 784–807.

[18] J. Korbecki, K. Kojder, D. Simińska, R. Bohatyrewicz, I. Gutowska, D. Chlubek, et al., CC Chemokines in a tumor: a review of pro-cancer and anti-cancer properties of the ligands of receptors CCR1, CCR2, CCR3, and CCR4, Int. J. Mol. Sci. 21 (21) (2020).

[19] Comprehensive molecular characterization of gastric adenocarcinoma, Nature 513 (7517) (2014) 202–209.

[20] N. Zhang, M. Cao, Y. Duan, H. Bai, X. Li, Y. Wang, Prognostic role of tumor-infiltrating lymphocytes in gastric cancer: a meta-analysis and experimental validation, Arch. Med. Sci. 16 (5) (2020) 1092–1103.

[21] Y. Oya, Y. Hayakawa, K. Koike, Tumor microenvironment in gastric cancers, Cancer Sci. 111 (8) (2020) 2696–2707.

[22] L. Greillier, P. Tomasini, F. Barlesi, The clinical utility of tumor mutational burden in non-small cell lung cancer, Transl. Lung Cancer Res. 7 (6) (2018) 639–646.